
Analysis Of Sea Surface Temperature Trends And Their Relationship With The Indian Ocean Dipole (IOD) In The Southern Waters Of Java During The 2000–2025 Period

Yenni Tri Ayundawati¹, Zahrani Salsabila², Citra Nur Ilahiyah³, Almer Beryl Adifta⁴, Nayadiva Shafinka⁵
^{1,2,3,4,5} Marine Science Program, Faculty of Fisheries and Marine Sciences, Universitas Padjadjaran, Jl. Ir. Sukarno
Km. 21, West Java, Indonesia

*Corresponding Author

E-mail: yenni22001@mail.unpad.ac.id

Abstract

Sea Surface Temperature (SST) is a key oceanographic parameter that regulates heat exchange between the atmosphere and the ocean; however, the current trend of global warming threatens thermal stability in tropical regions. This study aims to analyze long-term SST warming trends and identify their response and temporal relationship with the Indian Ocean Dipole (IOD) phenomenon in the southern waters of Java. A quantitative approach was applied using GLORYS12v1 ocean reanalysis data for the period 2000–2025, which were statistically analyzed using the Mann–Kendall test, Sen's Slope estimator, and lag correlation analysis. The results indicate a highly significant increasing trend in annual SST ($Z = 3.791$; $p = 0.000$) with a warming rate of $+0.0295^{\circ}\text{C}/\text{year}$. The highest mean SST occurred during the MAM season (29.17°C), while the lowest was observed during the JJA season (27.16°C). Regarding the IOD phenomenon, the Dipole Mode Index (DMI) and SST anomalies exhibited an inverse relationship with a correlation coefficient of $r = -0.47$ at a 0-month lag. Positive IOD phases were associated with SST cooling anomalies of up to -0.356°C , whereas negative IOD phases warmed the waters by up to 0.996°C . The consistent warming trend, combined with strong seasonal variability and a relatively weak response to IOD phases, suggests that SST dynamics are not solely controlled by the IOD. The findings demonstrate that the southern waters of Java have experienced significant ocean warming over the last two decades, while IOD variability plays a role in temporally modulating SST changes.

Keywords: Sea Surface Temperature, warming trend, Indian Ocean Dipole, lag correlation, GLORYS12v1, Southern Java.

INTRODUCTION

Sea Surface Temperature (SST) is a key oceanographic parameter that not only reflects the thermal condition of the upper ocean layer but also regulates heat exchange between the atmosphere and the ocean, evaporation patterns, and the distribution of rainfall above it (Vecchi & Soden, 2007). In recent decades, increasing global temperatures due to climate change have caused a more pronounced warming trend in various ocean regions, including the Indian Ocean. The oceans absorb most of the excess heat within the Earth's climate system; therefore, changes in SST have become one of the most important indicators for understanding the response of the marine environment to global climate change (IPCC, 2021).

Sea Surface Temperature (SST) is also a major component in the formation of the Indian Ocean Dipole (IOD) (Saji & Yamagata, 2003). This phenomenon is characterized by differences in SST anomalies between the western and eastern Indian Ocean, resulting in changes in regional atmospheric and oceanographic circulation patterns (Saji et al., 1999). During a positive IOD phase, the eastern Indian Ocean, including the waters surrounding Sumatra and Java, experiences relative cooling compared to normal conditions, while the western region undergoes warming (Saji et al., 1999; Cai et al., 2014). Conversely, the negative IOD phase is characterized by opposite conditions. According to Cai et al. (2014), the intensity and frequency of extreme IOD events tend to increase as a consequence of global warming. This situation leads to increasingly complex impacts on oceanographic and regional climatic conditions, including a higher frequency of marine heatwaves and sea level variations in the coastal regions of Indonesia (Holbrook et al., 2019).

The southern waters of Java represent a region that is highly sensitive to climate variability in the Indian Ocean due to their direct connection with the eastern Indian Ocean and their influence by the Asian–Australian monsoon system. Variations in Sea Surface Temperature (SST) in this region

are affected by interactions between atmospheric and oceanographic processes, including the Indian Ocean Dipole (IOD) phenomenon. Several studies have shown that Indonesian waters have experienced increasing occurrences of sea temperature anomalies and marine heatwaves over the past few decades (Iskandar et al., 2021; Han et al., 2022). These conditions indicate changes in the thermal characteristics of the ocean that require further investigation.

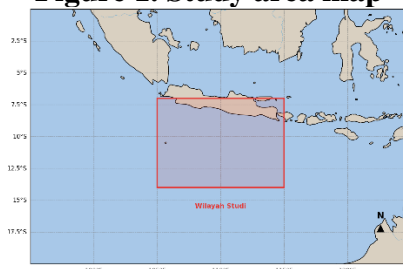
Although the influence of the IOD on oceanographic conditions in Indonesian waters has been widely studied, research focusing on long-term SST trends in the southern waters of Java and their relationship with IOD variability during the 2000–2025 period remains limited. This period encompasses several extreme IOD events as well as a substantial increase in global temperatures, both of which have the potential to influence the thermal dynamics of the region. Therefore, an analysis specifically evaluating SST trends, seasonal patterns, and their relationship with IOD variability in the southern waters of Java is essential to improve understanding of the region's thermal response to climate change and regional climate variability.

RESEARCH METHODS

Study Area

The study area covers the southern waters of Java, geographically bounded by 7°S–14°S latitude and 105°E–115°E longitude. The selection of these boundaries is based on the characteristics of the waters, which are influenced by local ocean currents such as the South Java Current and the Indonesian Throughflow (ITF), as well as by the climate variability associated with the Indian Ocean Dipole (IOD).

Figure 1. Study area map



Sea Surface Temperature Data

This study utilized Sea Surface Temperature (SST) data obtained from the GLORYS12v1 (Global Ocean Physics Reanalysis) Version 1 product developed by Mercator Ocean International and distributed through the Copernicus Marine Service (CMEMS; Product ID: GLOBAL_MULTIYEAR_PHY_001_030). GLORYS12v1 is a global oceanographic reanalysis product based on the NEMO (Nucleus for European Modelling of the Ocean) model with a horizontal resolution of approximately $0.083^\circ \times 0.083^\circ$ (Lellouche et al., 2021). The model assimilates observations from various sources, including satellite altimetry data, temperature and salinity measurements from Argo floats, multi-sensor satellite SST observations, as well as data from buoys and research vessels. The downloaded dataset covered the period from January 2000 to December 2025 with a daily temporal resolution.

Dipole Mode Index (DMI)

The DMI data used as an index of IOD intensity were obtained from the Japan Agency for Marine-Earth Science and Technology (JAMSTEC), which provides historical monthly DMI records based on the HadISST (Hadley Centre Sea Ice and SST) dataset. The DMI is calculated as the difference in SST anomalies between the western Indian Ocean (50°E–70°E, 10°S–10°N) and the southeastern Indian Ocean (90°E–110°E, 10°S–Equator) [4]. DMI values greater than $+0.4^\circ\text{C}$ indicate a positive IOD phase, values lower than -0.4°C indicate a negative IOD phase, and values between

-0.4°C and +0.4°C are classified as neutral conditions. Based on these criteria, IOD events during the period 2000–2025 were categorized into positive, negative, and neutral phases as shown in Table 1.

Table 1. IOD events during the period 2000–2025

IOD Phase	Event Years
Positive	2002, 2006, 2007, 2012, 2015, 2017, 2018, 2019, 2023
Negative	2010, 2016, 2022, 2025
Neutral	2000, 2001, 2003, 2004, 2005, 2008, 2009, 2011, 2013, 2014, 2020, 2021, 2024

Analysis Methods

SST Anomaly Analysis

Daily Sea Surface Temperature (SST) data were averaged into monthly values to generate a monthly SST time series. Based on these data, a monthly climatology for the period 2000–2019 was calculated by averaging SST values for the same month throughout the observation period. SST anomalies were then calculated by subtracting the corresponding climatological monthly mean from the monthly SST value. Mathematically, SST anomalies were calculated using the following equation: $SST' = SST_t - \bar{SST}(2000-2019)$ Where SST' is the sea surface temperature anomaly (°C), SST_t is the SST value at time t (month), and $\bar{SST}(2000-2019)$ is the average SST over the specified period. This method was applied to remove the seasonal component so that SST variability associated with climate phenomena such as the IOD could be observed more clearly.

Trend Analysis

Daily SST data were averaged into monthly values for the period 2000–2025. Two approaches were applied to identify trends: SST trends based on actual SST values and SST anomaly trends. SST trend analysis was conducted using three statistical approaches: Mann–Kendall, Sen’s Slope, and Ordinary Least Squares (OLS).

The Mann–Kendall test was used to detect the presence or absence of statistically significant trends in time-series data. This method is non-parametric and does not require the assumption of normal data distribution. Trend significance was determined based on a p-value threshold of 0.05. First, the value of S was calculated using the following equation (Aditya et al., 2021):

$$S = \sum_{i=1}^{n-1} \sum_{j=i+1}^n \text{sign}(x_j - x_i), \text{sign}(x_j - x_i)$$

Where Type equation here measures the initial strength of a trend by comparing all data pairs in the time series. If a value is greater than the previous value, the score is +1; if smaller, the score is -1; and if equal, the score is 0.

The variance of S was then calculated to determine whether the trend was significant:

$$\text{Var}(S) = \frac{n(n-1)(2n+5) - \sum_{i=1}^m t_i(t_i-1)(2t_i-5)}{18}$$

$$Z = \frac{S \pm 1}{\sqrt{\text{Var}(S)}}$$

A positive Z value indicates an increasing trend, whereas a negative Z value indicates a decreasing trend. Sen’s Slope was used together with the Mann–Kendall test. While the Mann–Kendall test determines trend significance, Sen’s Slope quantifies the magnitude of the trend. It estimates the trend rate in units of °C/year and is robust against outliers because it calculates the median slope of all possible data pairs. The Sen’s Slope equation is as follows (Aditya et al., 2021):

$$Q_i = \frac{(x_j - x_i)}{j - i}, 1 = 1, 2, 3, \dots, N$$

Where x_j and x_i represent data values at times j and i , respectively. Each observation series yields $N = n(n-1)/2$ slope estimates. As a comparison, Ordinary Least Squares (OLS) linear regression

was also applied to estimate trend rates, coefficients of determination (R^2), and statistical significance. The OLS equation is expressed as:

$$\hat{y} = a \cdot t + b$$

Where \hat{y} is the SST value, t is time, a is the rate of change (slope), and b is the intercept. OLS results were compared with Sen's Slope estimates to validate trend consistency.

Pearson Correlation

The relationship between SST anomalies and the Dipole Mode Index (DMI) was analyzed using Pearson correlation. This analysis was performed to identify the strength and direction of the linear relationship between the two variables. The correlation coefficient (r) ranges from -1 to $+1$, where positive values indicate a positive relationship, negative values indicate an inverse relationship, and values close to zero indicate a weak or absent linear relationship.

The Pearson correlation coefficient was calculated using the following equation:

$$R = \frac{\sum_{i=1}^n (t_i - \bar{t})(y_i - \bar{y})}{\sqrt{\sum_{i=1}^n (t_i - \bar{t})^2 \cdot \sum_{i=1}^n (y_i - \bar{y})^2}}$$

Where t_i is the time value at observation i , y_i is the SST anomaly at observation i , \bar{t} is the mean time value, \bar{y} is the mean SST anomaly, and n is the number of observations. This correlation function measures the strength and direction of the linear relationship between the two variables.

Lag correlation analysis was subsequently performed by applying temporal shifts (time lags) between the IOD index and SST anomaly data to identify response delays in SST to changes in IOD conditions. Time shifts are represented as t , where $t = 0$ indicates a relationship within the same period, $t > 0$ indicates that SST anomaly responses occur after changes in the IOD index, and $t < 0$ indicates that SST anomaly changes occur before changes in the IOD index. The lag value producing the maximum correlation coefficient was used to determine the dominant response time between the IOD index and SST anomalies.

Composite Analysis

Composite analysis was used to identify differences in SST anomaly characteristics during each phase of the Indian Ocean Dipole (IOD), namely positive, negative, and neutral phases. IOD phases were classified based on Dipole Mode Index (DMI) values, where the positive phase was defined as $DMI \geq +0.4^\circ\text{C}$, the negative phase as $DMI \leq -0.4^\circ\text{C}$, and values between these thresholds were categorized as neutral conditions.

After classification, SST anomaly data within each category were averaged to generate composite patterns representing SST characteristics during each IOD phase. The results of this analysis were used to examine SST changes and responses associated with variations in IOD intensity within the study area.

RESULTS AND DISCUSSION

Sea Surface Temperature Characteristics in the Southern Waters of Java

The seasonal distribution of Sea Surface Temperature (SST) in the southern waters of Java during the 2000–2025 period is shown in Figure 2, representing the four main seasonal phases: the west monsoon (DJF), the first transition season (MAM), the east monsoon (JJA), and the second transition season (SON). The analysis indicates that SST exhibits a clear seasonal cycle with considerable variability among seasons.

The highest SST distribution occurred during the MAM season, while the lowest values were observed during JJA. During DJF, SST conditions were relatively warm, ranging from 28.2 – 29.4°C with an average value of 28.98°C . In MAM, SST distribution became more homogeneous and reached the annual maximum temperature, with an average of 29.17°C (Table 2). In contrast, JJA showed a

significant decrease in SST, ranging from 26.6–27.2°C with an average of 27.16°C, where cooling was more pronounced along the southern coastal waters of Java. During SON, SST increased again, with temperatures around 26.6–27.0°C still observed in the southwestern part of the study area, while the eastern and southeastern regions reached approximately 27.8–28.0°C, resulting in an average SST of 27.48°C. These seasonal patterns indicate strong SST variability in the southern waters of Java, characterized by warmer conditions during transition seasons and cooler conditions during the east monsoon season.

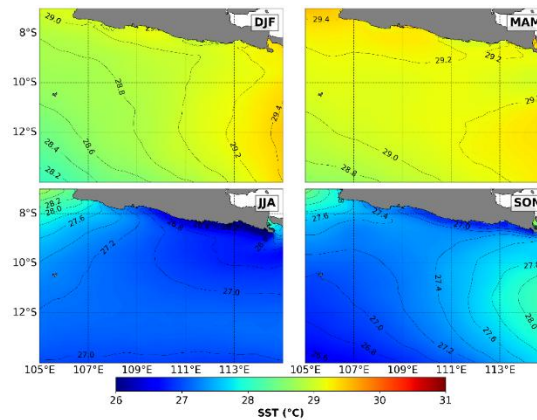


Figure 2. Seasonal spatial distribution of SST in the southern waters of Java during 2000–2025

Table 2. Seasonal average SST values during 2000–2025

Season	Mean SST (°C)	Minimum SST (°C)	Maximum SST (°C)
DJF	28.98	28.09	29.86
MAM	29.17	28.62	30.52
JJA	27.16	25.55	28.74
SON	27.48	26.49	30.18

Seasonal SST variability in the southern waters of Java is influenced by the dynamics of the Asian–Australian monsoon system, which controls ocean–atmosphere interactions, including changes in surface heat flux and upper-ocean circulation (Sprintall et al., 2014; Alfarizi et al., 2023). During the southeast monsoon, stronger winds enhance latent heat loss from the ocean surface, resulting in SST cooling (Alfarizi et al., 2023). Conversely, during transition seasons, weaker wind conditions favor heat accumulation in the upper ocean, leading to higher SST values (Wirasatriya et al., 2020). These processes demonstrate the important role of monsoon variability in regulating SST fluctuations in the southern waters of Java through its influence on surface heat fluxes and upper-layer mixing processes.

Sea Surface Temperature Trend Analysis (2000–2025)

The annual SST trend analysis for the period 2000–2025 (Figure 3) shows that the mean SST in the study area was 28.16°C. The Mann–Kendall test produced a Z value of 3.791 with a p-value of 0.000, indicating a statistically significant increasing SST trend at a confidence level exceeding 99%. The Sen’s Slope estimator indicates a warming rate of +0.0295°C year⁻¹. Over the 25-year observation period, SST is estimated to have increased cumulatively by approximately +0.74°C, demonstrating a consistent long-term ocean warming trend.

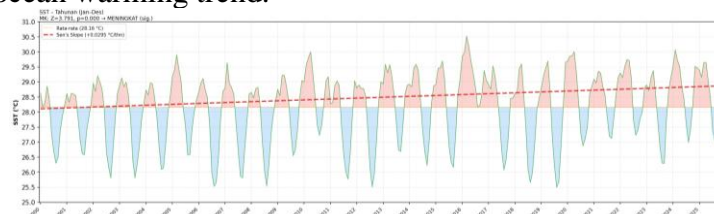


Figure 3. SST trend in the southern waters of Java during 2000–2025

Seasonal SST trend analysis revealed positive warming trends across all seasons, although with varying magnitudes. During DJF, SST increased by $0.0365^{\circ}\text{C year}^{-1}$, equivalent to approximately 0.91°C over 25 years, with a statistically significant trend ($p = 0.000$; $R^2 = 0.247$). An even stronger warming trend occurred during MAM, where the average SST reached 29.16°C and the warming rate was $0.0459^{\circ}\text{C year}^{-1}$, corresponding to about 1.15°C during the study period. The significance of these trends suggests persistent warming associated with increased solar energy input and seasonal atmospheric changes in tropical regions.

The highest warming rate was observed during SON, reaching $0.0561^{\circ}\text{C year}^{-1}$ or approximately 1.40°C over 25 years, with a significant trend ($p = 0.002$; $R^2 = 0.114$). In contrast, JJA exhibited the lowest warming rate of $0.0327^{\circ}\text{C year}^{-1}$ and did not show a statistically significant trend ($p = 0.058$; $R^2 = 0.047$). This indicates that interannual variability remains more dominant than long-term warming during this season. The relatively weak SST increase during JJA is closely related to seasonal upwelling events along the southern coast of Java induced by strengthened southeast monsoon winds. Upwelling brings colder subsurface water masses to the surface, thereby reducing SST and suppressing warming during the JJA season (Demi et al., 2020; Gunawan & Wibowo, 2024).

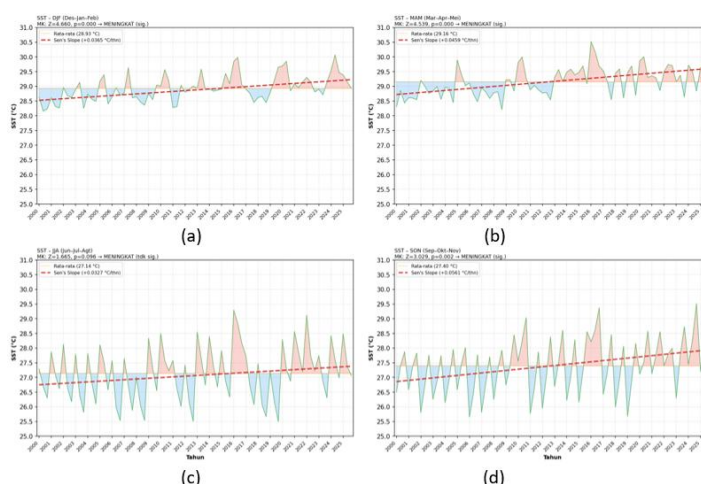


Figure 4. Seasonal SST trends in the southern waters of Java during 2000–2025: (a) DJF, (b) MAM, (c) JJA, and (d) SON

Table 3. Seasonal SST trend values during 2000–2025

Season	Slope ($^{\circ}\text{C year}^{-1}$)	Intercept	R^2	p-value	Significance
DJF	+0.0365	+0.0381	0.2466	0.0000	*
MAM	+0.0459	+0.0409	0.2314	0.0000	*
JJA	+0.0327	+0.0350	0.0466	0.0577	–
SON	+0.0561	+0.0552	0.1137	0.0025	*

Based on the SST anomaly warming-rate analysis during 2000–2025 (Figure 5), the lowest anomaly values were recorded during 2000–2002, reaching approximately -1.5°C , indicating SST conditions below the climatological average. SST anomalies gradually increased over time with a more fluctuating pattern. Conversely, the highest SST anomalies occurred during 2015–2016, reaching approximately $+1.8^{\circ}\text{C}$, representing the strongest ocean warming event throughout the observation period.

The Mann–Kendall trend analysis further confirmed the increasing SST tendency during 2000–2025. The Z statistic reached 8.605 with a p-value of 0.000, indicating a highly significant warming trend. The Sen’s Slope estimate of $+0.0312^{\circ}\text{C year}^{-1}$ suggests that SST increased on average by approximately 0.03°C annually. These findings indicate a persistent ocean warming process, where SST conditions at the end of the observation period were substantially warmer than those at the beginning.

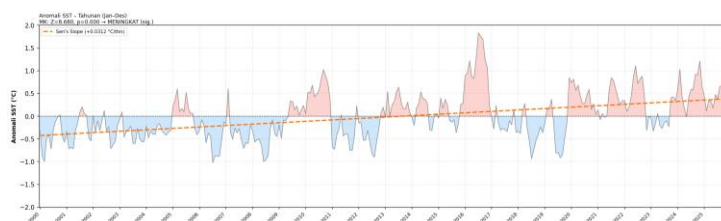


Figure 5. Temporal SST anomaly trend in the southern waters of Java during 2000–2025

The transition from predominantly negative anomalies toward predominantly positive anomalies reflects a shift in SST conditions over the study period. During the early years (2000–2008), SST anomalies were mostly negative, whereas after 2012 positive anomalies became increasingly frequent and intense. This pattern is evident from the growing occurrence and magnitude of positive anomalies toward the end of the study period. Such conditions may be associated with global warming driven by greenhouse gas emissions, which trap heat within the atmosphere and contribute to marine heatwave formation (Syaifullah, 2015). The accumulation of heat in the atmosphere subsequently increases both land surface temperatures and sea surface temperatures.

Relationship Between IOD and SST

During the 2000–2025 period (Figure 6), several Indian Ocean Dipole (IOD) events occurred. Positive IOD phases were recorded in 2002, 2006, 2007, 2012, 2015, 2017, 2018, 2019, and 2023, whereas negative IOD phases occurred in 2010, 2016, 2022, and 2025. The remaining years (2000, 2001, 2003, 2004, 2005, 2008, 2009, 2011, 2013, 2014, 2020, 2021, and 2024) were classified as neutral conditions.

The lag-correlation analysis between the DMI and SST anomalies over the 26-year period (Table 4) yielded a maximum correlation coefficient of $r = -0.47$ at lag 0 months. This result indicates an inverse relationship between DMI and SST anomalies, whereby increasing DMI values (positive IOD) are associated with decreasing SST anomalies, while decreasing DMI values (negative IOD) correspond to increasing SST anomalies in the southern waters of Java.

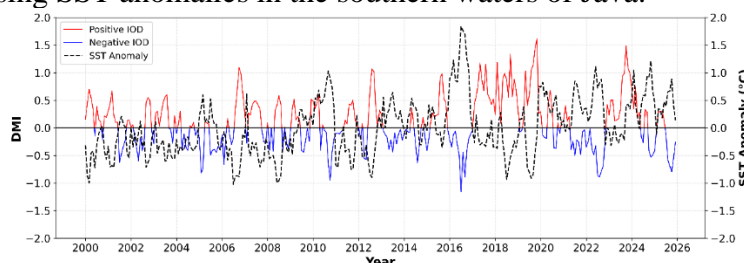


Figure 6. Temporal variation of the Dipole Mode Index (DMI) during 2000–2025

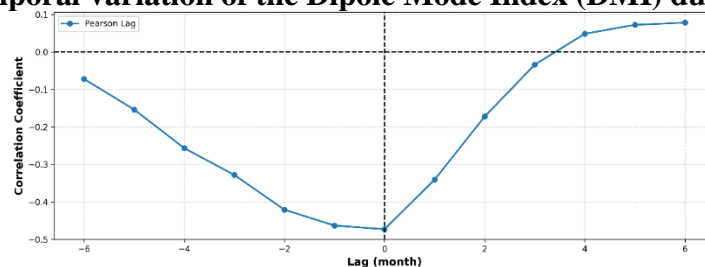


Figure 7. Lag-time correlation between DMI and SST during 2000–2025

SST Response to IOD Events

Based on the analysis of SST anomaly responses to IOD phases during 2000–2025 (Table 4), distinct SST anomaly characteristics were observed for each IOD phase. During positive IOD events, the mean SST anomaly was -0.356°C , with a correlation coefficient of $r = -0.047$ and a p-value of 0.748. Negative IOD phases produced a mean SST anomaly of 0.996°C , with $r = -0.187$ and $p = 0.489$. Meanwhile, neutral conditions showed a mean SST anomaly of 0.006°C , with $r = -0.284$ and $p = 0.00001$. Correlation coefficients across all phases indicate very weak relationships, as their values are close to zero and generally exhibit low statistical significance. These findings suggest that IOD

variability is not always the dominant factor controlling SST variations in the southern waters of Java and that other processes also contribute to SST dynamics.

Table 4. Correlation between DMI and SST during 2000–2025

IOD Phase	Mean SST Anomaly (°C)	Mean SST (°C)	Correlation Coefficient	p-value	Interpretation
Positive	-0.356	26.6	-0.047	0.74761	Very weak
Negative	0.996	28.0	-0.187	0.48906	Very weak
Neutral	0.006	27.1	-0.284	0.00001	Very weak

IOD events are characterized by differences in SST anomalies between the western and eastern Indian Ocean (Saji et al., 1999). During positive IOD phases, strengthened southeast winds enhance offshore Ekman transport, promoting the upwelling of colder subsurface waters that cool SST in the southern waters of Java (Wirasatriya et al., 2020). Conversely, during negative IOD phases, weakened southeast winds reduce water transport, allowing warm water masses to accumulate and increasing SST in the region.

These patterns indicate that changes in IOD phases influence the thermal characteristics of the ocean through modifications of atmospheric and oceanic conditions in the eastern Indian Ocean. However, the very low correlation coefficients across all phases suggest that the relationship between IOD and SST in the study area is relatively weak. This implies that SST variability during 2000–2025 was not controlled solely by IOD variability but also by various regional and seasonal factors. Consequently, changes in IOD phases do not always produce consistent SST responses, indicating that the influence of IOD on SST variability in the southern waters of Java remains limited. Tables and charts or captions are arranged in the form of a phrase (not a sentence) succinctly.

CONCLUSIONS

The results of this study demonstrate that the southern waters of Java experienced a significant long-term warming trend during the 2000–2025 period, with a Mann–Kendall statistic of $Z = 3.791$ ($p = 0.000$) and a warming rate of $+0.0295^{\circ}\text{C year}^{-1}$. Seasonal SST variability was strongly influenced by the Asian–Australian monsoon system, with the highest average SST occurring during the MAM season (29.17°C) and the lowest during JJA (27.16°C), when seasonal upwelling suppressed the warming rate. SST anomaly analysis revealed a shift from predominantly negative anomalies in the early years to predominantly positive anomalies in recent years, indicating a persistent ocean warming signal associated with global climate change.

Regarding the Indian Ocean Dipole (IOD), the relationship between the Dipole Mode Index (DMI) and SST anomalies showed an inverse correlation of $r = -0.47$ at lag 0 months. Positive IOD phases were associated with enhanced upwelling and cooling of SST anomalies to an average of -0.356°C , whereas negative IOD phases tended to increase SST anomalies. However, the weak correlations observed within each IOD phase indicate that SST variability in the southern waters of Java is not controlled solely by IOD dynamics. Other oceanographic and atmospheric factors, including monsoonal forcing, regional circulation, and air–sea interaction processes, also play important roles in modulating SST variability in the study area.

REFERENCES

- Aditya, F., Gusmayanti, E., & Sudrajat, J. (2021). Rainfall trend analysis using Mann-Kendall and Sen's slope estimator test in West Kalimantan. *IOP Conference Series: Earth and Environmental Science*, 893(1), 012006. <https://doi.org/10.1088/1755-1315/893/1/012006>
- Alfarizi, H., Wirasatriya, A., Kunarso, K., Abdillah, M. R., & Haryanti, D. (2023). Surface heat flux aspect on the variability of sea surface temperature and chlorophyll-a along the southern coast of Java. *Geographia Technica*, 18(1), 118–130. https://doi.org/10.21163/GT_2023.181.10
- Beliyana, E., Ningsih, N. S., Gunawan, S. R., & Tarya, A. (2023). Characteristics of marine heatwaves in the Indonesian waters during the PDO, ENSO, and IOD phases and their relationships to net surface heat flux. *Atmosphere*, 14(6), 1035. <https://doi.org/10.3390/atmos14061035>
- Cai, W., Santoso, A., Wang, G., Yeh, S. W., Annamalai, H., Cobb, K. M., Collins, M., Guilyardi, E., Jin, F. F., Kug, J. S., Lengaigne, M., McPhaden, M. J., Takahashi, K., Timmermann, A., Vecchi, G., Watanabe, M., & Wu, L. (2014). Increased frequency of extreme Indian Ocean Dipole events due to greenhouse warming. *Nature*, 510(7504), 254–258. <https://doi.org/10.1038/nature13327>
- Demi, L. A., Waas, H. J. D., Sarianto, D., & Haris, R. B. K. (2020). Karakteristik oseanografi pada daerah penangkapan ikan tuna di Samudra Hindia bagian timur Indonesia. *Jurnal Ilmu-Ilmu Perikanan dan Budidaya Perairan*, 15(1), 48–62. <https://doi.org/10.31851/7amw3x09>
- Gunawan, I., & Wibowo, N. S. (2024). Analisis variabilitas termoklin di perairan Indonesia dan dampaknya terhadap ekosistem laut. *Journal of Knowledge and Collaboration*, 1(4), 123–131. <https://doi.org/10.59613/rfmq7e07>
- Han, W., Vialard, J., McPhaden, M. J., Lee, T., Masumoto, Y., Feng, M., de Ruijter, W. P. M., & Sprintall, J. (2022). Sea level extremes and compounding marine heatwaves in coastal Indonesia. *Nature Communications*, 13(1). <https://doi.org/10.1038/s41467-022-34003-3>
- Holbrook, N. J., Scannell, H. A., Sen Gupta, A., Benthuisen, J. A., Feng, M., Oliver, E. C. J., Alexander, L. V., Burrows, M. T., Donat, M. G., Hobday, A. J., Moore, P. J., Thomsen, M. S., Wernberg, T., & Smale, D. A. (2019). A global assessment of marine heatwaves and their drivers. *Nature Communications*, 10(1). <https://doi.org/10.1038/s41467-019-10206-z>
- Intergovernmental Panel on Climate Change (IPCC). (2021). *Climate change 2021: The physical science basis. Contribution of Working Group I to the Sixth Assessment Report of the Intergovernmental Panel on Climate Change*. Cambridge University Press.
- Iskandar, M. R., Ismail, M. F. A., Arifin, T., & Chandra, H. (2021). Marine heatwaves of sea surface temperature off South Java. *Heliyon*, 7(12), e08618. <https://doi.org/10.1016/j.heliyon.2021.e08618>
- Kasim, F., Kalaka, S. R., Habibie, S. A., & Sau, M. J. (2026). Tren suhu permukaan laut, anomali ekstrem, dan keterkaitannya dengan ENSO di Teluk Tomini dan perairan sekitarnya periode 2003–2025. *Indonesian Journal of Oceanography*, 8(1), 22–35. <https://doi.org/10.14710/ijoce.v8i1.30633>
- Lellouche, J.-M., et al. (2021). *The Copernicus global 1/12° oceanic and sea ice reanalysis*. <https://doi.org/10.5194/egusphere-egu21-14961>
- Saji, N. H., & Yamagata, T. (2003). Structure of SST and surface wind variability during Indian Ocean Dipole mode events: COADS observations. *Journal of Climate*, 16(16), 2735–2751. [https://doi.org/10.1175/1520-0442\(2003\)016<2735:SOSASW>2.0.CO;2](https://doi.org/10.1175/1520-0442(2003)016<2735:SOSASW>2.0.CO;2)
- Saji, N. H., Goswami, B. N., Vinayachandran, P. N., & Yamagata, T. (1999). A dipole mode in the tropical Indian Ocean. *Nature*, 401(6751), 360–363. <https://doi.org/10.1038/43854>
- Sprintall, J., Gordon, A. L., Koch-Larrouy, A., Lee, T., Potemra, J. T., Pujiana, K., & Wijffels, S. E. (2014). The Indonesian seas and their role in the coupled ocean–climate system. *Nature Geoscience*, 7(7), 487–492. <https://doi.org/10.1038/ngeo2188>

- Syaifullah, M. D. (2015). Suhu permukaan laut perairan Indonesia dan hubungannya dengan pemanasan global. *Jurnal Segara*, 11(2), 103–113. <https://doi.org/10.15578/segara.v11i2.7356>
- Tong, B., Zhou, W., & Wang, X. (2025). Rising warm positive Indian Ocean Dipole under global warming: Early western Indian Ocean warming as a key predictor. *One Earth*, 8(4), 101277. <https://doi.org/10.1016/j.oneear.2025.101277>
- Tresnawati, R., et al. (2024). Long-term sea surface temperature prediction for Indonesian seas using multi-time-series satellite data for upwelling dynamics projection. *Remote Sensing Applications: Society and Environment*, 33, 101117. <https://doi.org/10.1016/j.rsase.2023.101117>
- Vecchi, G. A., & Soden, B. J. (2007). Global warming and the weakening of the tropical circulation. *Journal of Climate*, 20(17), 4316–4340. <https://doi.org/10.1175/JCLI4258.1>
- Wirasatriya, A., et al. (2020). Ekman dynamics variability along the southern coast of Java revealed by satellite data. *International Journal of Remote Sensing*, 41(21), 8475–8496. <https://doi.org/10.1080/01431161.2020.1797215>